

## Shell Analysis Using a Solid-Shell Approach

Pedro Ygor Rodrigues Mesquita<sup>1</sup>, Evandro Parente Junior<sup>1</sup>, João Batista Marques de Sousa Junior<sup>1</sup>, Elias Saraiva Barroso<sup>1</sup>

<sup>1</sup>*Laboratório de Mecânica Computacional e Visualização (LMCV), Departamento de Engenharia Estrutural e Construção Civil, Universidade Federal do Ceará  
Campus do Pici, Bloco 727, 60440-900, Fortaleza/Ceará, Brazil  
pedro.ygor@alu.ufc.br, evandro@ufc.br, joaobatistasousajr@ufc.br, elias.barroso@ufc.br*

**Abstract.** This work presents a general displacement-based formulation for analysis of shell structures using the solid-shell approach. In this approach, the element geometry is defined by the bottom and top surfaces, with a linear interpolation in the thickness direction. The presented formulation can be applied to develop isoparametric and isogeometric solid-shell elements. Unlike the traditional shell formulations, only translational degrees of freedom are required and a 3D constitutive model can be used. The performance of linear and quadratic elements is assessed using numerical examples.

**Keywords:** Shells, Solid-shell approach, Finite Element Method.

### 1 Introduction

Shells are structures whose thickness is much smaller than their other dimensions. They can exhibit an initial curvature, which is their main difference compared to plates. This type of structure is widely used in various sectors, such as in reservoirs and silos in civil construction, ship hulls, airplane fuselages, among other applications.

This work focus on the study of the solid-shell approach, in which the upper and lower faces of the shell are modeled, and a linear interpolation along the thickness is performed to define its geometry [1]. This approach adopts the hypothesis that the straight lines normal to the mid-surface of the shell remain straight, but not necessarily normal to the mid-surface after deformation [2]. Although this hypothesis is equivalent to the Reissner-Mindlin theory, the solid-shell approach only uses translational degrees of freedom, just like a solid, but with a lower computational cost due to the use of a smaller number of nodes.

In general, structural analysis using the solid-shell approach results in partial differential equations, whose analytical solutions are complex, making it necessary to adopt numerical methods to obtain approximate solutions. The Finite Element Method (FEM) is the most commonly used method for structural analysis and it will be used as an initial computational implementation. Isogeometric Analysis (IGA) was recently proposed by Hughes et al.[3] as an alternative method to FEM, which it is intended to be used in future work. Both formulations involve dividing the structure into a mesh with elements of finite dimensions.

The main difference is that in the FEM formulation, polynomial functions are used to interpolate the displacements of the elements, describing their geometry approximately through the isoparametric formulation. In contrast, IGA adopts an inverted sequence, where displacements are approximated by the basis functions that define the structure's geometry, such as B-Splines and NURBS (Non-Uniform Rational B-Splines), which are used in software that employs CAD (Computer-Aided Design) systems for geometric modeling. Thus, one of its major advantages is the consideration of the exact geometry of the problem.

This work presents the formulation of isoparametric elements based on the solid-shell for the structural analysis of plates and shells. This formulation can be applied in the implementation of finite elements using polynomial shape functions or isogeometric elements based on NURBS basis functions.

This paper is organized as follows. Section 2 discusses the solid-shell approach as well as its isoparametric formulation and the equilibrium equations of the problem. Section 3 shows some numerical examples where the present formulation is evaluate. Lastly, Section 4 exhibits the final considerations about the study.

## 2 Solid-Shell Approach

In the solid-shell approach, the geometry of the shell is defined by a surface on the top face and another surface on the bottom face, as shown in Figure 1, where a linear interpolation is assumed through the thickness [4]:

$$\mathbf{X}(\xi, \eta, \zeta) = \bar{\mathbf{X}}(\xi, \eta) + \zeta \mathbf{D}(\xi, \eta) \quad (1)$$

where  $\xi, \eta$  and  $\zeta$  are the parametric coordinates of the shell, which are defined in  $[-1, 1]$ ,  $\bar{\mathbf{X}}$  is the position vector on the mid-surface of the shell and  $\mathbf{D}$  is the director vector in the undeformed configuration. They are given by:

$$\bar{\mathbf{X}}(\xi, \eta) = \frac{1}{2} (\mathbf{X}^t(\xi, \eta) + \mathbf{X}^b(\xi, \eta)), \quad \mathbf{D}(\xi, \eta) = \frac{1}{2} (\mathbf{X}^t(\xi, \eta) - \mathbf{X}^b(\xi, \eta)) \quad (2)$$

in which the superscripts  $t$  and  $b$  are referred to top and bottom respectively. Similarly, the displacement can be calculated assuming a linear interpolation along the thickness:

$$\mathbf{u}(\xi, \eta, \zeta) = \bar{\mathbf{u}}(\xi, \eta) + \zeta \mathbf{d}_u(\xi, \eta) \quad (3)$$

where  $\bar{\mathbf{u}}$  is displacement vector on the mid-surface of the shell and  $\mathbf{d}_u$  is the displacement director vector, which are computed as:

$$\bar{\mathbf{u}}(\xi, \eta) = \frac{1}{2} (\mathbf{u}^t(\xi, \eta) + \mathbf{u}^b(\xi, \eta)), \quad \mathbf{d}_u(\xi, \eta) = \frac{1}{2} (\mathbf{u}^t(\xi, \eta) - \mathbf{u}^b(\xi, \eta)) \quad (4)$$

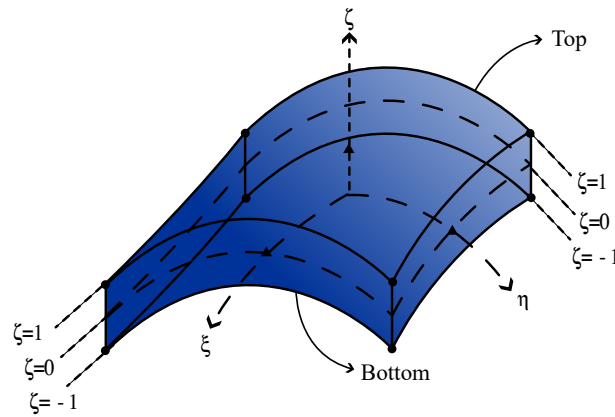


Figure 1. Solid-shell geometry.

Considering small displacements, the strains can be written as:

$$\boldsymbol{\varepsilon} = \begin{Bmatrix} \varepsilon_x \\ \varepsilon_y \\ \varepsilon_z \\ \gamma_{xy} \\ \gamma_{xz} \\ \gamma_{yz} \end{Bmatrix} = \begin{Bmatrix} u_{,x} \\ v_{,y} \\ w_{,z} \\ u_{,y} + v_{,x} \\ w_{,x} + u_{,z} \\ v_{,z} + w_{,y} \end{Bmatrix} \quad (5)$$

Assuming the linear elastic behavior, the constitutive relations can be given by Hooke's Law, where a 3D constitutive model is used [5]:

$$\boldsymbol{\sigma} = \mathbf{C} \boldsymbol{\varepsilon} \quad (6)$$

### 2.1 Discretization

Using the solid-shell approach, the shell is modeled by two surfaces, each of which can be represented by a linear combination of  $mn$  shape functions  $R_i$  used in the displacement interpolation and the nodes with coordinates

$(X_i, Y_i, Z_i)$  on the upper and lower faces:

$$\begin{Bmatrix} X^t \\ X^b \end{Bmatrix} = \sum_{i=1}^{nn} R_i \begin{Bmatrix} X_i^t \\ X_i^b \end{Bmatrix}, \quad \begin{Bmatrix} Y^t \\ Y^b \end{Bmatrix} = \sum_{i=1}^{nn} R_i \begin{Bmatrix} Y_i^t \\ Y_i^b \end{Bmatrix}, \quad \begin{Bmatrix} Z^t \\ Z^b \end{Bmatrix} = \sum_{i=1}^{nn} R_i \begin{Bmatrix} Z_i^t \\ Z_i^b \end{Bmatrix} \quad (7)$$

the geometry of the isoparametric solid-shell element is determined by performing a linear interpolation of the nodes' coordinates along the thickness, substituting Equation (7) into Equation (1):

$$\mathbf{X} = \begin{Bmatrix} X \\ Y \\ Z \end{Bmatrix} = \sum_{i=1}^{nn} R_i \bar{\mathbf{X}}_i + \zeta \sum_{i=1}^{nn} R_i \mathbf{D}_i = \frac{1}{2} \sum_{i=1}^{nn} (1 + \zeta) R_i \begin{Bmatrix} X_i^t \\ Y_i^t \\ Z_i^t \end{Bmatrix} + \frac{1}{2} \sum_{i=1}^{nn} (1 - \zeta) R_i \begin{Bmatrix} X_i^b \\ Y_i^b \\ Z_i^b \end{Bmatrix} \quad (8)$$

By further developing this expression, the following equation is obtained:

$$\mathbf{X} = \sum_{i=1}^{nn} N_i^t \begin{Bmatrix} X_i^t \\ Y_i^t \\ Z_i^t \end{Bmatrix} + \sum_{i=1}^{nn} N_i^b \begin{Bmatrix} X_i^b \\ Y_i^b \\ Z_i^b \end{Bmatrix} \quad (9)$$

where:

$$N_i^t(\xi, \eta, \zeta) = \frac{1}{2}(1 + \zeta) R_i(\xi, \eta) \quad \text{and} \quad N_i^b(\xi, \eta, \zeta) = \frac{1}{2}(1 - \zeta) R_i(\xi, \eta) \quad (10)$$

The isoparametric approach uses the same basis functions that describe the geometry to approximate the displacements of the shell:

$$\mathbf{u} = \begin{Bmatrix} u \\ v \\ w \end{Bmatrix} = \sum_{i=1}^{nn} R_i \bar{\mathbf{u}}_i + \zeta \sum_{i=1}^{nn} R_i \mathbf{d}_{ui} = \sum_{i=1}^{nn} N_i^t \begin{Bmatrix} u_i^t \\ v_i^t \\ w_i^t \end{Bmatrix} + \sum_{i=1}^{nn} N_i^b \begin{Bmatrix} u_i^b \\ v_i^b \\ w_i^b \end{Bmatrix} = \mathbf{N} \mathbf{d} \quad (11)$$

where  $\mathbf{d} = \{u_i^t, v_i^t, w_i^t, u_i^b, v_i^b, w_i^b\}^T$  is the vector of degrees of freedom of the problem (only displacements of nodes on the upper and lower surfaces), and  $\mathbf{N}$  is the displacement approximation matrix:

$$\mathbf{N} = [\mathbf{N}_1 \quad \mathbf{N}_2 \quad \dots \quad \mathbf{N}_{nn}] \quad (12)$$

In which each submatrix is associated with the projection of the  $i$ -th node of the lower and upper faces, which can be calculated as:

$$\mathbf{N}_i = \begin{bmatrix} N_i^t & 0 & 0 & N_i^b & 0 & 0 \\ 0 & N_i^t & 0 & 0 & N_i^b & 0 \\ 0 & 0 & N_i^t & 0 & 0 & N_i^b \end{bmatrix} \quad (13)$$

The relationship between strains and displacements is obtained by substituting Equation (11) into Equation (5):

$$\boldsymbol{\varepsilon} = \sum_{i=1}^{nn} \begin{bmatrix} N_{i,x}^t & 0 & 0 & N_{i,x}^b & 0 & 0 \\ 0 & N_{i,y}^t & 0 & 0 & N_{i,y}^b & 0 \\ 0 & 0 & N_{i,z}^t & 0 & 0 & N_{i,z}^b \\ N_{i,y}^t & N_{i,x}^t & 0 & N_{i,y}^b & N_{i,x}^b & 0 \\ N_{i,z}^t & 0 & N_{i,x}^t & N_{i,z}^b & 0 & N_{i,x}^b \\ 0 & N_{i,z}^t & N_{i,y}^t & 0 & N_{i,z}^b & N_{i,y}^b \end{bmatrix} \begin{Bmatrix} u_i^t \\ v_i^t \\ w_i^t \\ u_i^b \\ v_i^b \\ w_i^b \end{Bmatrix} = \mathbf{B} \mathbf{d} \quad (14)$$

Since the assembly of the stiffness matrix requires the definition of the  $\mathbf{B}$  matrix, which includes the first-order derivatives of the basis functions with respect to the Cartesian axes, it is necessary to perform a transformation

from the parametric space to the Cartesian space. Thus, the Jacobian matrix is defined:

$$\mathbf{J} = \begin{bmatrix} X_{,\xi} & Y_{,\xi} & Z_{,\xi} \\ X_{,\eta} & Y_{,\eta} & Z_{,\eta} \\ X_{,\zeta} & Y_{,\zeta} & Z_{,\zeta} \end{bmatrix} = \begin{bmatrix} \sum N_{i,\xi}^t X_i^t + N_{i,\xi}^b X_i^b & \sum N_{i,\xi}^t Y_i^t + N_{i,\xi}^b Y_i^b & \sum N_{i,\xi}^t Z_i^t + N_{i,\xi}^b Z_i^b \\ \sum N_{i,\eta}^t X_i^t + N_{i,\eta}^b X_i^b & \sum N_{i,\eta}^t Y_i^t + N_{i,\eta}^b Y_i^b & \sum N_{i,\eta}^t Z_i^t + N_{i,\eta}^b Z_i^b \\ \sum N_{i,\zeta}^t X_i^t + N_{i,\zeta}^b X_i^b & \sum N_{i,\zeta}^t Y_i^t + N_{i,\zeta}^b Y_i^b & \sum N_{i,\zeta}^t Z_i^t + N_{i,\zeta}^b Z_i^b \end{bmatrix} \quad (15)$$

Thus, the relationship between the derivatives of the basis functions in the parametric system and the derivatives in the Cartesian system is defined:

$$\begin{Bmatrix} N_{i,x}^t \\ N_{i,y}^t \\ N_{i,z}^t \end{Bmatrix} = \mathbf{J}^{-1} \begin{Bmatrix} N_{i,\xi}^t \\ N_{i,\eta}^t \\ N_{i,\zeta}^t \end{Bmatrix} \quad \text{and} \quad \begin{Bmatrix} N_{i,x}^b \\ N_{i,y}^b \\ N_{i,z}^b \end{Bmatrix} = \mathbf{J}^{-1} \begin{Bmatrix} N_{i,\xi}^b \\ N_{i,\eta}^b \\ N_{i,\zeta}^b \end{Bmatrix} \quad (16)$$

## 2.2 Equilibrium equations

According to the Principle of Virtual Work (PVW), equilibrium occurs when the virtual internal work ( $\delta U$ ) equals the virtual external work ( $\delta W_{ext}$ ) for any admissible virtual displacements ( $\delta \mathbf{u}$ ) at any point, provided they are small and respect the boundary conditions of the system, as described below:

$$\delta U = \delta W_{ext} \Rightarrow \int_V \delta \boldsymbol{\varepsilon}^T \boldsymbol{\sigma} dV = \int_V \delta \mathbf{u}^T \mathbf{b} dV + \int_S \delta \mathbf{u}^T \mathbf{q} dS + \sum_{j=1}^n \mathbf{u}_j^T \mathbf{F}_j \quad (17)$$

where  $\delta \boldsymbol{\varepsilon}$  is the virtual strain vector,  $\mathbf{b}$  are the body forces,  $\mathbf{q}$  are the distributed loads, and  $\mathbf{F}_j$  are the concentrated loads at point  $j$ .

Thus, Equation (17) can be rewritten in terms of nodal displacements, such that the stiffness matrix of the isoparametric element  $\mathbf{K}_e$  can be calculated by substituting the strains with Equation (14):

$$\delta U = \int_V \delta \boldsymbol{\varepsilon}^T \mathbf{C} \boldsymbol{\varepsilon} dV = \delta \mathbf{d}^T \int_V \mathbf{B}^T \mathbf{C} \mathbf{B} dV \mathbf{d} \Rightarrow \mathbf{K}_e = \int_V \mathbf{B}^T \mathbf{C} \mathbf{B} dV \quad (18)$$

The external force vector can also be calculated in terms of nodal displacements  $\mathbf{u}$  from the virtual external work:

$$\delta W_{ext} = \delta \mathbf{d}^T \int_V \mathbf{N}^T \mathbf{b} dV + \delta \mathbf{d}^T \int_S \mathbf{N}^T \mathbf{q} dS + \delta \mathbf{d}^T \sum_{j=1}^n \mathbf{N}_j^T \mathbf{p}_j = \delta \mathbf{d}^T \mathbf{f}_e \quad (19)$$

in which:

$$\mathbf{f}_e = \int_V \mathbf{N}^T \mathbf{b} dV + \int_S \mathbf{N}^T \mathbf{q} dS + \sum_{j=1}^n \mathbf{N}_j^T \mathbf{F}_j \quad (20)$$

From the stiffness matrix and the external force vector of the element, the Direct Stiffness Method (DSM) is used where each term is added to the corresponding degree of freedom in the global stiffness matrix  $\mathbf{K}$  and external force vector  $\mathbf{f}$  of the structure. This way, the global displacements of the shell can be found by solving the system:

$$\mathbf{K} \mathbf{d} = \mathbf{f} \quad (21)$$

Finally, it is important to know that the shape functions  $R_i$  used to describe in-plane geometry and displacement approximation can be defined by NURBS functions for IGA or shape functions of plane finite elements for FEM. In this work, as an initial implementation, the shape functions considered are those from Q4 and Q8 plane elements [6], which are used to form the solid-shell elements called SOLIDS8 and SOLIDS16 respectively. These elements were implemented in the software FAST (Finite Element Analysis Tool), developed in C++ programming language using object-oriented programming (OOP) techniques.

## 3 Numerical Examples

This section presents the results obtained using the isoparametric solid-shell approach for linear static analysis of plates. In order to assess and verify the formulation and its computer implementation, these results are compared with analytical solutions and the results achieved by 3D continuum finite elements.

The proposed element severely suffer from different types of locking, such as shear and Poisson locking [7]. Thus, this work also evaluates the influence of the integration scheme to alleviate the locking problem. The full integration scheme uses  $p + 1$  Gauss points in each element in-plane direction and 2 points along the thickness, and the reduced integration uses  $p$  points in the plane directions and 2 points along the thickness. The suffixes F and R are adopted for full and reduced integration respectively. The quadratic 3D element with 20 nodes (BRICK20) [6] is used for comparison.

### 3.1 Example 1 - Slender cantilever beam

This example deals with the static analysis of a cantilever beam subjected to a moment (Case 1) and a transversal load (Case 2) at its free end. The material properties, geometry, boundary conditions and loading can be seen in Figure 2. It is important to note that the structure is very slender, with  $h/L = 1/2000$ . The moment of  $M = 10^{-3}$  is applied by line forces and the transverse load  $P = -10^{-3}$  by a distributed force on the free face.

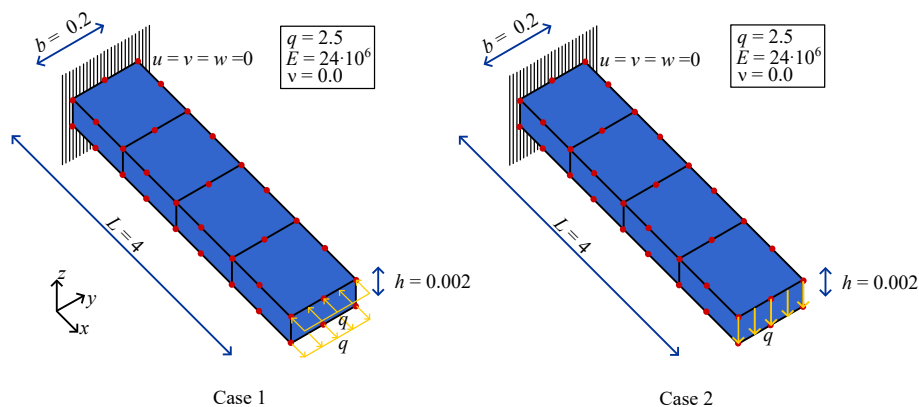


Figure 2. Problem definition and  $4 \times 1 \times 1$  SOLIDS16 mesh ( $nn = 46$ ).

The tip deflections obtained by the analytical solution using Timoshenko beam theory in the cases 1 and 2 are  $w_{ref} = 2.500$  and  $w_{ref} = -6.667$  respectively [8], considering  $M = 10^{-3}$  and  $P = -10^{-3}$ . Figure 3 shows the convergence study with mesh refinement. The results of SOLIDS8F are not shown due to the poor results obtained with relative error about 100%, as well as BRICK20R, which presents a spurious (hourglass) mode. The reduced integration scheme for SOLIDS8 presents good results and convergence in both cases. In case 1, SOLIDS16F shows better convergence and results, while in case 2 SOLIDS16R shows faster convergence than SOLIDS16F, but worse accuracy for refined meshes. BRICK20F element seems to have locked more than the others in both cases.

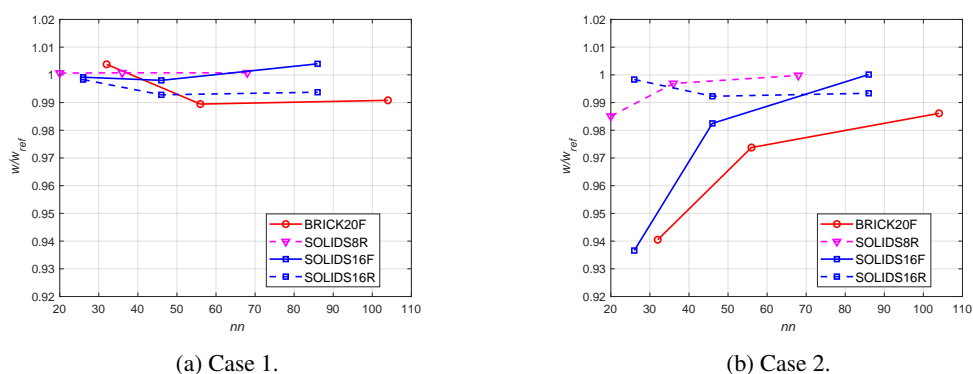


Figure 3. Convergence study of the cantilever beam.

### 3.2 Example 2 - Square plate under uniform load

This example presents the static analysis of clamped square plates subjected to uniform transversal load. Figure 4 shows the material properties, geometry, boundary conditions and loading.

The deflections are compared to the reference solution  $w_{ref} = -2.458 \times 10^{-7}$ ,  $-2.172 \times 10^{-4}$ , and  $-2.169 \times 10^{-1}$

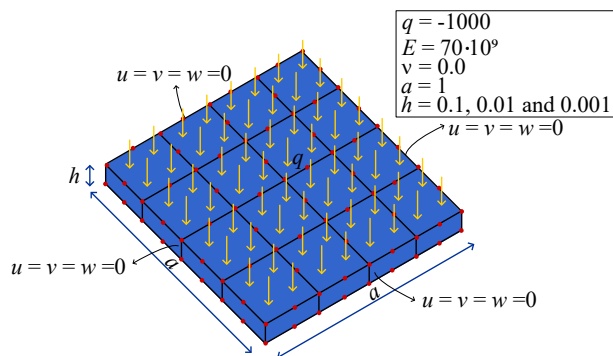


Figure 4. Problem definition and 4x4x1 SOLIDS16 mesh ( $nn = 130$ ).

for  $h/a = 1/10, 1/100$  and  $1/1000$  respectively, obtained using a fine mesh of Reissner-Mindlin plate elements. Figure 5 presents the convergence study with mesh refinement for the different length-to-thickness ratios.

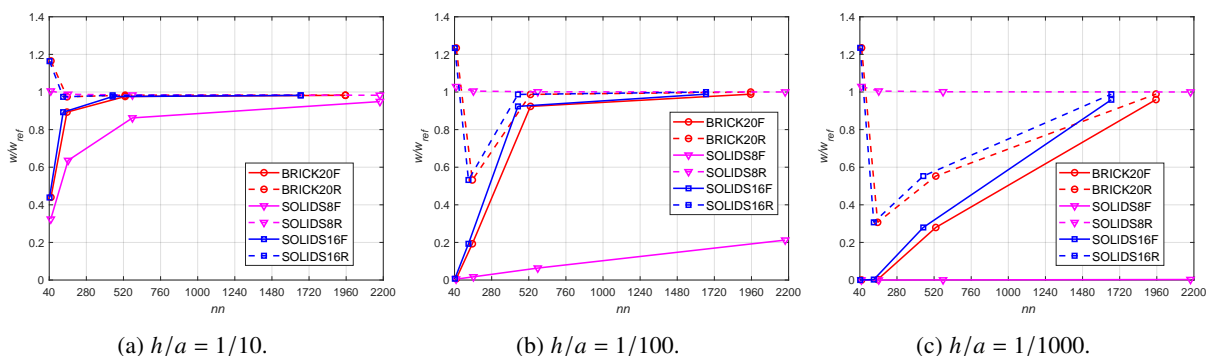


Figure 5. Convergence study of the square plates for  $\nu = 0$ .

Firstly, it can be noted that the smaller the length-to-thickness ratio, the slower the convergence, which shows the presence of the locking problem. The reduced integration scheme for SOLIDS8 presents better convergence and results than the full integration in all cases. SOLIDS8F only presents relatively good result in  $h/a = 1/10$  and it tends to lock more as the slenderness increases, presenting relatively errors about 100% for  $h/a = 1/1000$ . SOLIDS16R shows better convergence and slightly larger displacements than SOLIDS16F. In general, both solid-shell elements with 8 and 16 nodes converged to a similar result in all cases. BRICK20R exhibits better convergence than BRICK20F, but analogous converged results.

Now Poisson’s ratio is considered  $\nu = 0.3$  and the central deflections are compared to the reference solution  $w_{ref} = -2.347 \times 10^{-7}, -1.978 \times 10^{-4}$  and  $-1.974 \times 10^{-1}$  for  $h/a = 1/10, 1/100,$  and  $1/1000$  respectively also obtained using Reissner-Mindlin plate elements. Figure 6 shows the convergence study with mesh refinement for the different  $h/a$  ratios.

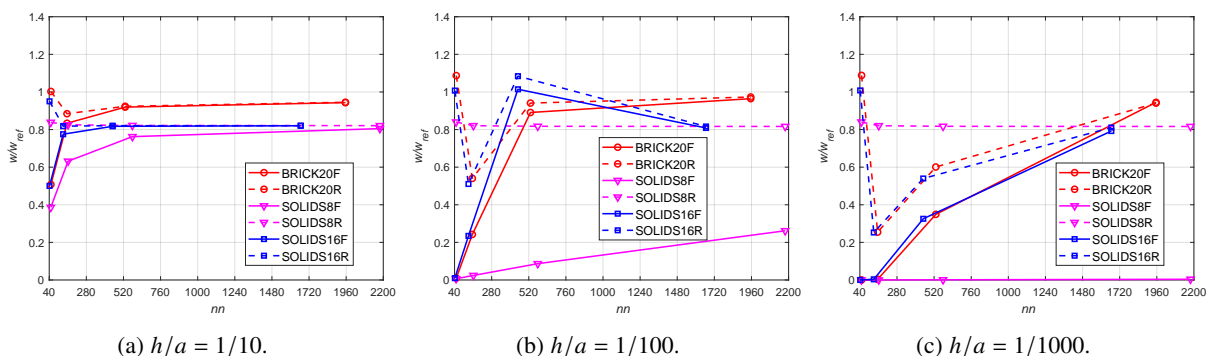


Figure 6. Convergence study of the square plates for  $\nu = 0.3$ .

It can be seen that for all  $h/a$  cases, the displacements of SOLIDS8 and SOLIDS16 elements seem to have locked with full and reduced integration. Since the only aspect that changed was the consideration of Poisson’s

ratio, this is an instance of the so-called Poisson locking [7]. The results for BRICK20 element with full and reduced integration schemes remain consistent compared with the Figure 6, suggesting that it does not suffer from Poisson locking.

## 4 Conclusion

This work presented a general displacement-based formulation using the solid-shell approach for analysis of plates and shells. As an initial work, the shape functions of Q4 and Q8 plane isoparametric elements with a linear shape function through the thickness were used to interpolate the displacement field and the geometry, resulting in the SOLIDS8 and SOLIDS16 elements. Since this approach presents locking problems, the reduced integration scheme was adopted as a technique to alleviate it.

The numerical examples showed that the use of SOLIDS8 elements with full integration scheme presents poor results in all cases, and the reduced integration can improve them in general. The use of SOLIDS16 elements did not show better convergence than SOLIDS8, but their converged results were closer to the reference deflections. Nevertheless, the reduced integration had not the same effect in SOLIDS16 as in SOLIDS8. In general, the shear locking was alleviated by the reduced integration technique, but the same benefit did not occurred for the Poisson locking, making further investigations necessary.

This work presented the initial part of an ongoing research, which aims to incorporate a NURBS-based isogeometric approach as well as to expand the solid-shell formulation to buckling, free vibration and nonlinear analysis of free form shells.

**Acknowledgements.** The authors gratefully acknowledge the financial support provide by CNPq (Conselho Nacional de Desenvolvimento Científico e Tecnológico).

**Authorship statement.** The authors hereby confirm that they are the sole liable persons responsible for the authorship of this work, and that all material that has been herein included as part of the present paper is either the property (and authorship) of the authors, or has the permission of the owners to be included here.

## References

- [1] H. Parisch. A continuum-based shell theory for non-linear applications. *International Journal for Numerical Methods in Engineering*, vol. 38, n. 11, pp. 1855–1883, 1995.
- [2] R. Hauptmann and K. Schweizerhof. A systematic development of ‘solid-shell’ element formulations for linear and non-linear analyses employing only displacement degrees of freedom. *International Journal for Numerical Methods in Engineering*, vol. 42, n. 1, pp. 49–69, 1998.
- [3] T. J. Hughes, J. A. Cottrell, and Y. Bazilevs. Isogeometric analysis: Cad, finite elements, nurbs, exact geometry and mesh refinement. *Computer Methods in Applied Mechanics and Engineering*, vol. 194, pp. 4135–4195, 2005.
- [4] L. Leonetti, F. Liguori, D. Magisano, and G. Garcea. An efficient isogeometric solid-shell formulation for geometrically nonlinear analysis of elastic shells. *Computer Methods in Applied Mechanics and Engineering*, vol. 331, pp. 159–183, 2018.
- [5] K. Bathe. *Finite Element Procedures in Engineering Analysis*. Prentice-Hall civil engineering and engineering mechanics series. Prentice-Hall, 1982.
- [6] R. D. Cook, D. S. Malkus, M. E. Plesha, and R. J. Witt. *Concepts and Applications of Finite Element Analysis*. John Wiley Sons, inc., 2002.
- [7] J. Zhi and T.-E. Tay. Explicit modeling of matrix cracking and delamination in laminated composites with discontinuous solid-shell elements. *Computer Methods in Applied Mechanics and Engineering*, vol. 351, pp. 60–84, 2019.
- [8] C. M. Wang. Timoshenko beam-bending solutions in terms of euler-bernoulli solutions. *Journal of Engineering Mechanics*, vol. 121, n. 6, pp. 763–765, 1995.